

# Semi-analytical model of acoustic-wave generation by a laser line pulse in an optically absorptive isotropic cylinder

D Ségur<sup>1</sup>, A L Shuvalov<sup>1</sup>, Y Pan<sup>2</sup>, B Audoin<sup>1</sup>

<sup>1</sup> Laboratoire de Mécanique Physique, UMR CNRS 8469, Université Bordeaux 1, 33405 Talence, France

<sup>2</sup> Institute of Acoustics, Tongji University, Shanghai, China

E-mail: d.segur@lmp.u-bordeaux1.fr

**Abstract.** Semi-analytical model for calculating acoustic response to a line-focused laser pulse in an optically absorptive isotropic cylinder is proposed and implemented. It is assumed that the laser input is absorbed over the volume and thus creates a radially distributed thermoelastic source. Closed-form solution is obtained in the Fourier domain. Two inverse Fourier transforms in frequency and circumferential wave number yield the sought waveforms of acoustic response in the time-space domain. Numerical simulation is compared to the calculation based on a surface dipole source. The two signals have essentially different shapes of the wave-arrival peaks when the optical penetration is large enough.

Keywords: laser ultrasonics, distributed thermoelastic source, acoustic response, cylinder

## 1. Introduction

The laser ultrasonics technique is a unique tool for acoustic-wave generation in objects with a curved surface. Much work has been done by this means for generating surface and bulk acoustic waves in opaque cylindrical targets with a view of their non-destructive testing and evaluation, see recent publications [1–4] and the bibliography therein. There exists a well developed theory for the case when, at a given laser wavelength, the target (either cylindrical or planar) is opaque and hence the source is located at the surface. Given so, the ablation model applies for high enough local energy such that causes ablation at the laser-heated region of the surface, and the dipole (Scruby’s) model applies for relatively low incoming energy [5]. In this latter, thermoelastic regime, the dilatation of an infinitely

small volume adjacent to the surface produces a surface source equivalent to a force dipole. The dipole strength has been derived in [6, 7].

Thermoelastic regime for the optically absorptive materials implies that the laser input penetrates into a target and creates a volume distribution of sources therein. Hence the assumption of a surface source is no longer appropriate. Laser generation of acoustic waves in optically absorptive materials has been considered for the case of a planar target (plate) [8]. The next natural step is extending laser ultrasonics treatment to optically absorptive cylindrical targets. To the best of the authors' knowledge, such a case has not yet been studied. The present paper proposes a two-dimensional (2D) semi-analytical model for calculating acoustic response to a line-focused laser pulse in an optically absorptive isotropic cylinder. Thermoelastic regime of generation is assumed and a typical case of materials with negligible thermal conductivity is treated. Closed-form solution is obtained in the Fourier domain to the inhomogeneous ordinary differential system with a radially distributed thermoelastic source and with the traction-free boundary condition at the cylinder surface. Performing two inverse Fourier transforms yields the sought waveforms of acoustic response in the time-space domain. This calculation is carried out in the paper for two different source settings. One of them formally treats the case of an opaque cylinder by assuming a vanishingly small optical penetration or, which is equivalent, a buried source tending to the cylinder surface. The other considers the actual case of an optically absorptive cylinder, where the exponentially decaying law of optical absorption produces a distributed source with large enough radial penetration length. The results obtained for these two settings are compared with the calculation based on Scruby's model of a surface dipole source. It is observed that the waveforms, computed for a buried source tending to the surface, agree very well with those following for Scruby's surface-source model, whereas the waveforms, computed for a distributed source, have essentially different shapes comparatively to the prediction following for the surface source. The former observation serves as a test for our model, while the latter highlights the effect of laser-energy penetration into the bulk of an optically absorptive cylinder.

## 2. Background

Consider an infinite homogenous isotropic elastic cylinder of radius  $R$ , whose surface is heated by the line-focused laser pulse independent of the axial coordinate  $z$ . The laser energy is supposed to be low enough to preclude ablation. It is assumed that viscoelasticity, thermal conduction and the contribution of deformation to the entropy change may be disregarded. The thermoelastic generation of acoustic wave is therefore described by the following simplified system of governing equations:

$$\nabla \cdot \sigma = \rho \ddot{\mathbf{u}}; \quad \sigma = \lambda \text{tr}(\varepsilon) \mathbf{I} + 2\mu \varepsilon - \beta T \mathbf{I}; \quad \rho c_p \dot{T} = q, \quad (1)$$

where  $\sigma$  is the stress tensor including mechanical and thermal stresses,  $\varepsilon$  is the strain tensor,  $\mathbf{u}$  is the displacement,  $\rho$  is the density,  $\lambda$  and  $\mu$  are the Lamé coefficients,  $\beta = (3\lambda + 2\mu) \alpha_T$  is the thermal modulus ( $\alpha_T$  is the dilatation coefficient),  $T$  is the temperature rise,  $c_p$  is the specific heat,  $q$  is the power density of the line laser source,  $\mathbf{I}$  is the identity matrix and  $\text{tr}$  denotes the trace.

The heat input  $q(r, \theta, t)$  creates a volume distribution of thermal sources inside the cylinder through the optical absorption. Assuming normal incidence of the Gaussian laser beam [9] and the exponential fall off of the incoming energy  $E$ , it follows that

$$q(r, \theta, t) = \alpha E g(\theta) \delta(t) e^{-\alpha(R-r)}, \quad (2)$$

where

$$g(\theta) = \frac{1}{\gamma} \sqrt{\frac{4 \ln 2}{\pi}} e^{-(4 \ln 2) \frac{\theta^2}{\gamma^2}}, \quad \gamma = 2 \arctan \frac{b}{2R} \quad (3)$$

describes the angular extent of the beam with width  $b$ . By (1)<sub>3</sub> and (2),

$$T(r, \theta, t) = \frac{\alpha E}{\rho c_p} g(\theta) H(t) e^{-\alpha(R-r)}, \quad (4)$$

where  $H$  is the Heaviside function. The temperature field (4) specifies the thermal stress  $\sigma^{(T)} = -\beta T$  in (1).

Thus, the thermoelastic problem is reduced to solving the 2D plane-strain equation of motion for the displacement  $\mathbf{u}(r, \theta, t) = u_r \mathbf{e}_r + u_\theta \mathbf{e}_\theta$  in the cylinder cross-section  $(\mathbf{e}_r, \mathbf{e}_\theta)$ . Divergence of the thermal stress plays the role of a source term. The equation is complemented by the traction-free boundary condition (BC)  $\mathbf{e}_r \sigma = \mathbf{0}$  at the cylinder surface  $r = R$ .

### 3. Solution in the Fourier domain

#### 3.1. Setup

Consider the above 2D problem in the Fourier domain  $\{r, \nu, \omega\}$ , where  $\nu$  is the circumferential wave number and  $\omega$  the angular frequency. Thereafter in this section the factor  $e^{j(\nu\theta - \omega t)}$  is omitted, the same notations for the transformed functions are used, and their dependence on  $\nu, \omega$  is understood and suppressed. According to (1) and (4), we write

$$\begin{aligned} \sigma(r) &= \sigma^{(m)}(r) + \sigma^{(T)}(r) \mathbf{I}, \\ \sigma^{(m)}(r) &= \lambda \text{tr}[\varepsilon(r)] \mathbf{I} + 2\mu \varepsilon(r), \quad \sigma^{(T)}(r) = -\beta T_0 e^{-\alpha(R-r)}, \end{aligned} \quad (5)$$

where  $T_0 (\sim \alpha)$  involves double transform of (4) in  $\theta$  and  $t$ .

The equation of motion in the Fourier domain reduces to the ordinary differential system in  $\mathbf{u}(r)$  with the source term provided by  $\nabla \sigma^{(T)}(r)$ . Using Helmholtz decomposition, this equation may be re-cast in the form of two uncoupled Bessel equations for the longitudinal and shear elastic potentials  $\varphi(r)$  and  $\psi(r)$ ,

$$\begin{pmatrix} \nabla^2 + k_L^2 & 0 \\ 0 & \nabla^2 + k_T^2 \end{pmatrix} \begin{pmatrix} \varphi(r) \\ \psi(r) \end{pmatrix} = \begin{pmatrix} b e^{-\alpha(R-r)} \\ 0 \end{pmatrix}, \quad (6)$$

where  $k_L^2 = \rho \omega^2 / (\lambda + 2\mu)$ ,  $k_T^2 = \rho \omega^2 / \mu$  and  $b = \beta T_0 / (\lambda + 2\mu)$ . The traction-free BC, which couples  $\varphi(r)$  and  $\psi(r)$ , is

$$\begin{pmatrix} \sigma_{rr}^{(m)}(R) \\ \sigma_{r\theta}^{(m)}(R) \end{pmatrix} + \begin{pmatrix} -\beta T_0 \\ 0 \end{pmatrix} = \mathbf{0}, \quad (7)$$

where

$$\begin{pmatrix} \sigma_{rr}^{(m)}(R) \\ \sigma_{r\theta}^{(m)}(R) \end{pmatrix} = \mathbf{S}(R) \begin{pmatrix} \varphi(R) \\ \psi(R) \end{pmatrix}, \quad \mathbf{S}(r) = 2\mu \begin{pmatrix} \frac{\lambda}{2\mu} \nabla^2 + \frac{d^2}{dr^2} & \frac{j\nu}{r} \left( \frac{d}{dr} - \frac{1}{r} \right) \\ \frac{j\nu}{r} \left( \frac{d}{dr} - \frac{1}{r} \right) & \frac{1}{2} \nabla^2 - \frac{d^2}{dr^2} \end{pmatrix}. \quad (8)$$

For the future use, introduce the following abridged notations of the values taken at the boundary  $r = R$ :

$$K_{L,T} \equiv k_{L,T}R, \quad B_{T,L} \equiv \frac{K_{T,L}J'_\nu(K_{T,L})}{J_\nu(K_{T,L})}, \quad ' \equiv \left[ \frac{dJ_\nu(x)}{dx} \right]_{x=K_{L,T}}. \quad (9)$$

Note that expressing the results in terms of  $B_{T,L}$  is helpful for numerical implementation, because the exponential growth of the Bessel functions of the order  $\nu \gg K_{L,T}$  is avoided this way (see [10]).

### 3.2. Green function

First, we solve an auxiliary problem for a buried point source at  $r_0$  ( $0 \leq r_0 < R$ ) under the homogeneous BC on the mechanical stresses (see (8)<sub>1</sub>),

$$\begin{pmatrix} \nabla^2 + k_L^2 & 0 \\ 0 & \nabla^2 + k_T^2 \end{pmatrix} \begin{pmatrix} \Phi(r|r_0) \\ \Psi(r|r_0) \end{pmatrix} = \begin{pmatrix} bR^2 \frac{\delta(r-r_0)}{r} \\ 0 \end{pmatrix}, \quad \mathbf{S}(R) \begin{pmatrix} \Phi(R|r_0) \\ \Psi(R|r_0) \end{pmatrix}_{r_0 < R} = \mathbf{0}, \quad (10)$$

where the factor  $R^2$  in (10)<sub>1</sub> is added to merely keep physical dimensions intact. The partial solution to the given inhomogeneous Bessel equation on  $\Phi(r|r_0)$  is [11]

$$g(r|r_0) = bR^2 \frac{\pi}{2} [J_\nu(k_L r) Y_\nu(k_L r_0) H(r_0 - r) + Y_\nu(k_L r) J_\nu(k_L r_0) H(r - r_0)], \quad (11)$$

where  $J_\nu$  and  $Y_\nu$  are the Bessel functions of the first and second kind. Thus the solution to (10) is sought in the form

$$\begin{pmatrix} \Phi(r|r_0) \\ \Psi(r|r_0) \end{pmatrix} = \begin{pmatrix} g(r|r_0) + C_\Phi(r_0) J_\nu(k_L r) \\ C_\Psi(r_0) J_\nu(k_T r) \end{pmatrix}, \quad (12)$$

where  $J_\nu(k_L r)$  and  $J_\nu(k_T r)$  are the solutions of the homogeneous Bessel equation on the potentials. Substituting (12) into the BC of (10) and appealing to (8)<sub>2</sub> provides an algebraic system of equations on the coefficients  $C_\Phi(r_0)$  and  $C_\Psi(r_0)$ . It has the form

$$\mathbf{S}(R) \begin{pmatrix} \Phi(R|r_0) \\ \Psi(R|r_0) \end{pmatrix}_{r_0 < R} = \frac{2\mu}{R^2} \left[ \mathbf{\Lambda} \begin{pmatrix} C_\Phi(r_0) \\ C_\Psi(r_0) \end{pmatrix} + bR^2 \frac{\pi}{2} J_\nu(k_L r_0) \gamma \right] = \mathbf{0} \quad (13)$$

with

$$\mathbf{\Lambda} = \begin{pmatrix} \left( \nu^2 - \frac{K_T^2}{2} - B_L \right) J_\nu(K_L) & j\nu(B_T - 1) J_\nu(K_T) \\ j\nu(B_L - 1) J_\nu(K_L) & - \left( \nu^2 - \frac{K_T^2}{2} - B_T \right) J_\nu(K_T) \end{pmatrix}, \quad (14)$$

$$\gamma = Y_\nu(K_L) \begin{pmatrix} \nu^2 - \frac{K_T^2}{2} - B_L^{(Y)} \\ j\nu(B_L^{(Y)} - 1) \end{pmatrix},$$

where the use of (9) has been made, and  $B_L^{(Y)}$  differs from  $B_L$  by replacing  $J_\nu$  with  $Y_\nu$ . Note that the matrix (first-rank tensor)  $\mathbf{\Lambda}$  results in (13) from applying the boundary stress operator  $\mathbf{S}(R)$  to the solutions of the homogeneous equation. Hence  $D = 0$ , where

$$D = \frac{\det \mathbf{\Lambda}}{J_\nu(K_L) J_\nu(K_T)} = -\nu^4 + \nu^2(B_L B_T + K_T^2 + 1) - \left(\frac{K_T^2}{2} + B_L\right) \left(\frac{K_T^2}{2} + B_T\right), \quad (15)$$

is the dispersion equation for the eigenmodes of the traction-free cylinder. By (13),

$$\begin{pmatrix} C_\Phi(r_0) \\ C_\Psi(r_0) \end{pmatrix} = -bR^2 \frac{\pi}{2} J_\nu(k_L r_0) \mathbf{\Lambda}^{-1} \gamma. \quad (16)$$

Inserting (16) along with (11) into (12) completes finding the solution  $\Phi(r|r_0)$  and  $\Psi(r|r_0)$  to (10).

### 3.3. Displacement for a distributed source

Once the solution  $\Phi(r|r_0)$  and  $\Psi(r|r_0)$  to (10) has been found, it remains to take its convolution with the radially distributed source  $\sim e^{-\alpha(R-r)}$  for obtaining the solution  $\varphi(r)$  and  $\psi(r)$  to Eq. (6), and to invoke Helmholtz decomposition  $\mathbf{u} = \nabla\varphi + \nabla \times (\psi \mathbf{e}_z)$  for finding  $\mathbf{u}(r)$ . Because these two are linear operations, they may be applied in the optional order. Thus

$$\mathbf{u}(r) = \frac{1}{R^2} \int_0^R \{ \nabla \Phi(r|r_0) + \nabla \times [\Psi(r|r_0) \mathbf{e}_z] \} e^{-\alpha(R-r_0)} r_0 dr_0, \quad (17)$$

where  $\mathbf{G}(r|r_0) = \nabla \Phi(r|r_0) + \nabla \times [\Psi(r|r_0) \mathbf{e}_z]$  is the displacement response to a buried source  $\nabla \sigma^{(T)}(r) \sim \nabla \frac{\delta(r-r_0)}{r}$ . Note that application of the boundary-stress differential operator to  $g(r|r_0)$  (see (12)) in the integrand of (17) taken with  $r, r_0 \rightarrow R$  provides an extra delta-function term, which compensates  $\sigma^{(T)}(R) = -\beta T_0$  in the BC (7) for the distributed source.

In the context of laser ultrasonics, the important particular case is the displacement at the surface  $r = R$ . It can be written in the following closed form:

$$\mathbf{u}(R) = \begin{pmatrix} u_r \\ u_\theta \end{pmatrix} = IU_0 \frac{K_L^2}{J_\nu(K_L)} \begin{pmatrix} \nu^2 - B_T - \frac{K_T^2}{2} \\ j\nu(1 - B_T) \end{pmatrix}, \quad (18)$$

where

$$I = \int_0^1 J_\nu(K_L x) e^{-\alpha R(1-x)} x dx \quad (x = r/R), \quad U_0 = \frac{\beta T_0 R}{2\mu D}, \quad (19)$$

and  $D$  is given in (15).

Numerical simulations in §4.2 involve the model case of a buried source located at  $r_0 = R - \epsilon$  tending to the surface. For this case,  $\mathbf{u}(R) = \frac{1}{R^2} \mathbf{G}(R|R - \epsilon)$  is given by (18) with  $I = J_\nu(K_L)$  (the equality is to within arbitrarily small  $\epsilon/R$ ). Obviously, this case may also be seen as a limit of vanishingly small optical penetration length  $\alpha^{-1}$ .

## 4. Numerical treatment and the simulation results

### 4.1. Inverse Fourier transform

2D Fourier transform, discrete in circumferential number  $\nu$  and continuous in frequency  $\omega$ , has next been performed to obtain the sought acoustic response in the time-space domain  $\{r, \theta, t\}$ . The calculation has been made for the radial component of response at the surface, which is most usually the quantity measured by the laser ultrasonics technique. Denote its above-derived value in the transform domain as  $u_r(R) = \hat{u}_r(R, \nu, \omega)$ , where  $u_r(R)$  is given by Eq.(18). Fast Fourier Transform algorithm in frequency has been applied, with a small imaginary part added to  $\omega$  ( $\omega^* = \omega - j\delta$  where  $\delta > 0$ , e.g. [12]) in order to avoid zeros of the dispersion equation  $D = 0$ , see (19) and the remark to (15). On taking Fourier transform in  $\nu$ , the use has been made of the fact that, by (18),  $\hat{u}_r(r, \nu, \omega)$  is an even function of  $\nu$ . As a result the sought response  $u_r(R, \theta, t)$  is described by the formula

$$u_r(R, \theta, t) = \frac{e^{-\delta t}}{\pi} \int_{-\infty}^{\infty} \left\{ \sum_{\nu=0}^{\infty} \varepsilon_{\nu} \hat{u}_r(R, \nu, \omega) \cos(\nu\theta) \right\} e^{-j\omega t} d\omega, \quad (20)$$

where  $\varepsilon_{\nu}$  is the Neumann factor equal to 1 if  $\nu = 0$  and to 2 otherwise.

The series in (20) is non-absolutely convergent [10]. Its convergence in  $\nu$  depends on  $\omega$  and hence so does the truncation order  $\nu_m$ , which is supposed to satisfy the criterion

$$\frac{|\hat{u}_r(R, \nu_m, \omega)|}{\sum_{\nu=0}^{\nu_m} |\hat{u}_r(R, \nu, \omega)|} < \varepsilon, \quad (21)$$

where  $\varepsilon$  is the error bound. It is, however, known that usually the sum in question is mainly due to the first terms of the sum. For the frequency band used in our case, it was verified that taking a fixed truncation order  $\nu_m$  such that keeps about 200 terms of the series ensures that the committed error does not exceed  $10^{-5}$ .

### 4.2. Results of numerical simulations

Numerical simulations have been implemented for the opaque aluminium rod and the optically absorptive NG5 coloured glass rod, both of the diameter 5 mm. The values of their elastic and thermal constants are listed in Table 1 (the notations are explained below (1)). Assuming the laser wavelength 355 nm, the absorption length for NG5 coloured glass is  $\alpha^{-1} = 0.8$  mm. The typical values of the laser beam-width  $b = 0.15$  mm and of the pulse duration 5 ns are taken. The radial component of the surface displacement  $u_r(R, \theta, t)$  is supposed to be detected at the point  $(r, \theta) = (R, \pi)$  which is diametrically opposite to the generation point  $(R, 0)$ . Fourier transform in  $\omega$  has been performed with the numerical parameter  $\delta = 0.035$ , see (20).

The results of numerical simulations are presented in Figs.1 and 2. The wave arrivals are marked by the dashed lines. They are identified and denoted according to the nomenclature proposed in [4] on the basis of a ray trajectory analysis. The notation  $nL$  and  $nT$  corresponds to the arrivals of longitudinal and transverse bulk modes, travelling along the straight diameter path and undergoing  $n$  normal reflections from the cylinder surface at the

**Table 1.** Physical properties of Al and NG5 glass used in simulations.

	$\rho$ [g cm <sup>-3</sup> ]	$\lambda$ [GPa]	$\mu$ [GPa]	$\alpha_T$ [K <sup>-1</sup> ]	$c_p$ [J kg <sup>-1</sup> K <sup>-1</sup> ]
Al	2.69	56	26.5	2.5e-6	902
NG5	2.31	17.4	22.9	6.5e-6	700

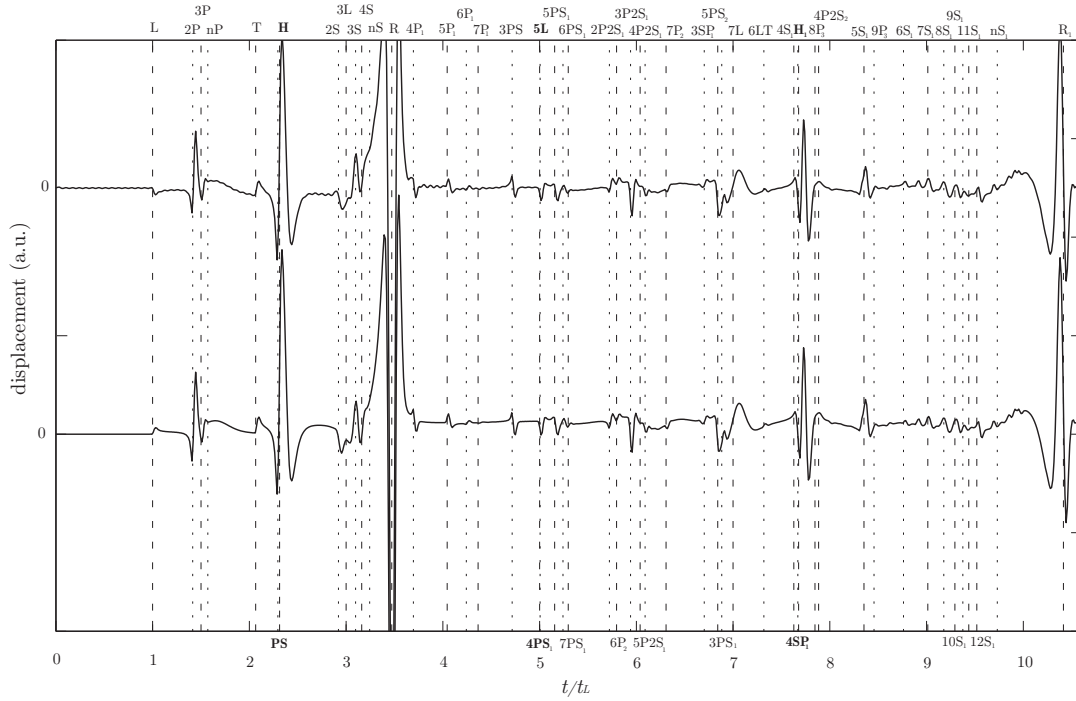
edge points. The notation  $nP$  and  $nS$  also corresponds to, respectively, the longitudinal and transverse bulk modes, but these ones arrive at the detection point after a broken path resulting from  $n$  oblique reflections without modal conversion. The wave arrivals, involving modal conversion at oblique reflections, are denoted by  $mPnS_r$ , where the subscript  $r$  is the number of round trips about the center made within the given path. The Rayleigh-wave arrival is denoted by  $R_r$ . The notation  $H_r$  is used for the wave arrival due to the head wave, i.e., due to the transverse mode radiated by the skimming longitudinal wave in the direction of the critical angle  $\varphi_c = \arcsin \sqrt{2\mu/(\lambda + 2\mu)}$ .

Fig.1 compares two simulations of the laser-generated acoustic response  $u_r(R, \pi, t)$  for the opaque aluminium cylinder. The upper curve is computed by means of the developed procedure reduced to the model case such that assumes a radially concentrated buried source tending to the cylinder surface or, equally, a vanishingly small optical penetration length (see the closing remark in § 3.3). The lower curve is computed by means of Scruby's model of the surface dipole source [5]. Precise agreement of the arrival times and waveform shapes of both signals is observed.

Fig.2 presents the numerical results for the optically absorptive NG5 coloured glass cylinder. The upper curve shows the acoustic response  $u_r(R, \pi, t)$  computed from Eqs. (18)-(20) for the radially distributed source, which takes into account marked enough optical penetration of the given material ( $\alpha R \approx 3$ ). This curve is again compared with the 'would-be' signal calculated for this case on the basis of Scruby's surface-source model (lower curve). It is seen that while the arrival times for both signals are obviously in good accordance, there is an evident discrepancy in the shape of the waveforms. For instance, the first longitudinal-wave arrival  $L$  on the upper curve has a characteristic bipolar broad shape, which is not observed on the lower curve. Another striking dissimilarity is that the bulk-wave and surface-wave arrivals on the upper curve have more or less similar amplitudes, which is in contrast to the predominant peaks of the first Rayleigh-wave arrivals  $R$  and  $R_1$  on the lower curve. Altogether, the difference between these two curves highlights the effect of optical penetration, which Scruby's surface-source model is not intended to describe.

## 5. Conclusions

Acoustic response of an isotropic cylinder to a laser line pulse has been simulated in the framework of 2D semi-analytical model, which takes into account optical penetration into the bulk of optically absorptive cylinder material. The waveforms calculated for the



**Figure 1.** Acoustic response of the aluminium rod computed for the model of a buried source tending to the surface (upper curve) and for Scruby's model of a surface source (lower curve). The notations for wave arrivals are explained in text.

aluminium rod with a vanishingly small penetration coincide, as expected, with those obtained from Scruby's model of a surface dipole source. At the same time, calculation for the glass rod with large enough penetration length has demonstrated an essential difference of the waveform shapes relatively to the signal calculated for the same material by way of the surface-source model.

The semi-analytical procedure developed in this paper paves the way to quantitative analysis of experimental results of laser ultrasonics generation in cylindrical samples made of optically absorptive materials. First experimental data have recently been obtained and will be reported elsewhere.

## References

- [1] Clorennec D, Royer D and Walaszek H 2002 *Ultrasonics* **40** 783 – 789
- [2] Clorennec D and Royer D 2003 *Appl. Phys. Lett.* **82** 4608–4610
- [3] Pan Y, Rossignol C and Audoin B 2003 *Appl. Phys. Lett.* **82** 4379–4381
- [4] Pan Y, Rossignol C and Audoin B 2004 *J. Acoust. Soc. Am.* **115** 1537–1545
- [5] Scruby C B and Drain L E 1990 *Laser Ultrasonics Technique & Applications* (Adam Hilger)



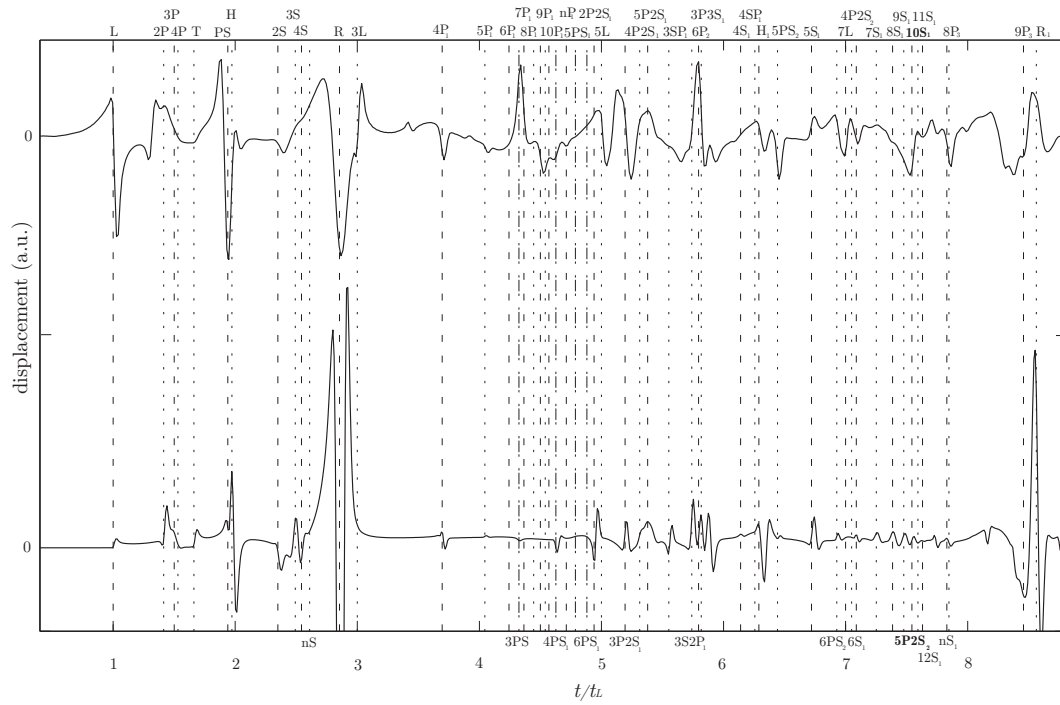


**Figure 2.** Acoustic response of the optically absorptive NG5 coloured glass rod. The upper curve is calculated for the radially distributed source taking into account optical penetration. The lower curve is calculated from Scruby's model of a surface source for opaque materials.

- [6] Royer D 2001 *Ultrasonics* **39** 345 – 354
- [7] Arias I and Achenbach J D 2003 *Int. J. Solids Struct.* **40** 6917 – 6935 special issue in Honor of George J. Dvorak
- [8] Dubois M, Enguehard F and Bertrand L 1994 *Phys. Rev. E* **50** 1548–1551
- [9] Hecht E 2002 *Optics* (San Fransisco: Addison Wesley)
- [10] Rousselot J L 1987 *La Diffusion Acoustique par des Cibles Elastiques de Formes Géométrique Simple: Théories et Expériences* ed Gespa N (Paris: CEDOCAR) chap 21
- [11] Kamke E 1971 *Differentialgleichungen: Lösungsmethoden und Lösungen* (New-York: Chelsea)
- [12] Weaver R L, Sachse W and Kim K Y 1996 *J. Appl. Mech.* **63** 337–346